Momentum Transfer Across Fluid-Fluid Interfaces in Porous Media: a Network Model

P. A. Goode and T. S. Ramakrishnan
Schlumberger-Doll Research, Ridgefield, CT 06877

Two-phase flow in porous media is described based on the extended form of Darcy's law, which ignores momentum transfer at fluid-fluid interfaces. Two forms of corrections to this simple description have been proposed in the literature: one on the relative permeability dependence on viscosity ratio; the other on the velocities assumed to be proportional to both phase pressure gradients and so introducing an additional saturation-dependent cross coefficient.

In this article, to identify the correct form of transport equations, a simple cubic network model of $30\times30\times30$ bonds is used. The cross section of the bonds is that of a four-cusp duct. The fluid interface in each duct is located by capillary equilibrium. The duct hydraulic conductances are then obtained as a function of viscosity ratio and phase volume fraction using a finite element calculation. These individual duct results are used in the network calculations for which a percolation algorithm is applied to simulate nonwetting phase displacing wetting phase, a process also known as initial drainage. Flow calculations show that both the nonwetting-phase relative permeability and the cross coefficient are strong functions of saturation and viscosity ratio. Also, the off-diagonal terms may contribute to a nonnegligible fraction of the flow. The proposed generalization of the Darcy equations is applicable to all problems involving multiphase flow in porous media. The current practices for relative permeability measurements and reservoir simulation may have to be reexamined in the context of the proposed transport equations.

Introduction

The slow steady flow of a single Newtonian fluid through a stationary, inert and isotropic porous medium is described by Darcy's law (Darcy, 1856):

$$v = -\lambda\frac{\Delta p}{l}, \tag{1}$$

where v is the superficial velocity, p is the fluid pressure, and l is the length of the porous medium along the direction of macroscopic flow. λ is a proportionality constant referred to as mobility and may be rewritten as (Nutting, 1930):

$$\lambda = \frac{k}{\mu}, \tag{2}$$

where μ is the shear coefficient of viscosity, and k is the *permeability* of the medium and is independent of the fluid properties. In Eq. 1 we have ignored body forces, and throughout this article we shall assume that these forces are negligible. For general applicability, a differential form of Eq. 1:

$$v = -\frac{k}{\mu}\nabla p \tag{3}$$

is often employed (Scheidegger, 1974).

Many practical applications such as oil recovery processes and unsaturated moisture movement in soils involve simultaneous movement of two immiscible fluids. Under steady conditions, in which the fractional volume of the void space occupied by each of the phases (saturation) also does not change with location, each fluid is assumed to have its own channels

Correspondence concerning this article should be addressed to T. S. Ramakrishnan.

of flow. Also, for a given direction of saturation change, the channels are presumed unique for each saturation (see, for example, Bear, 1972). Therefore, Eq. 1 is extended to the steady flow of two fluids with a saturation-dependent permeability for each phase. These "effective" permeability functions account for the reduced flow area as well as the increased torusity in the flow paths due to the presence of the second fluid. Also, under such steady conditions, a pressure difference exists between the two phases, which from a macroscopic point of view, will be uniform across the sample. The pressure difference is in the *capillary* pressure, p_c, and is a function of the saturation alone. In other words, it will change from one steady state to another. A conceptual experiment to illustrate this is presented by Marle (1981).

Although the extension of Eq. 1 to steady flow of two liquids is important conceptually, it is not very useful for a practical problem. Therefore, a heuristic extension of the steady-state form for unsteady conditions is written as:

$$v_i = -\lambda_i(S_w)\,\nabla p_i, \tag{4}$$

where the subscript $i = w, n$ is used to indicate properties of preferentially wetting and nonwetting phases, respectively. S_w is the local wetting phase saturation and λ_i is the phase i mobility. It is given by:

$$\lambda_i = \frac{k k_{ri}(S_w)}{\mu_i}, \tag{5}$$

where the saturation-dependent function k_{ri} is known as *relative permeability*. kk_{ri} is the effective permeability to phase i at the saturation of interest. To complete the statement of two-phase Darcy equations, it is also assumed that "local capillary equilibrium" exists between the two phases:

$$p_n - p_w = p_c(S_w). \tag{6}$$

The two-phase Darcy equations in the form of Eqs. 4–6 were put down by Leverett (1940), although the concept of saturation-dependent permeability dates back to Buckingham (1907). Numerous authors have contributed to the development of the concepts as well as the laboratory measurements of the permeabilities (Richards, 1931; Wyckoff and Botset, 1936; Muskat and Meres, 1936; Hassler et al., 1936; Muskat et al., 1937; Leverett, 1939; Leveret and Lewis, 1941). In all of the above work and in most of what is practiced today, relative permeabilities are assumed to be functions of saturation alone as long as the velocity of the fluids are sufficiently small, the change of saturation is monotonic, and if the medium is ideal, that is, it is isotropic, uniform and homogeneous (see, for example, Bear, 1972; Scheidegger, 1974; Barenblatt et al., 1990). These restrictive assumptions regarding flow rates, monotonic saturation changes, and the ideality of the medium will be taken for granted throughout the rest of this article. Since Eqs. 4–6 rely on the assumption that Darcy's law applies to each of the fluids, they require that each fluid be bounded only by the solid or that the fluid-fluid drag at interfaces is negligibly small. Although this may be true if pores have no corners or roughness and if the contact angle is finite, it is not necessarily true in general. Therefore, Rose (1972) conjectured the following correction to the two-phase Darcy equations:

$$v_w = -\lambda_{ww}\nabla p_w - \lambda_{wn}\nabla p_n \tag{7}$$

$$v_n = -\lambda_{nn}\nabla p_n - \lambda_{nw}\nabla p_w, \tag{8}$$

where Rose (1972), in analogy with the thermodynamics of irreversible processes (Callen, 1960) assumed that:

$$\lambda_{wn} = \lambda_{nw}. \tag{9}$$

The cross-term mobility thus may be denoted simply as λ_c. We may then define a cross coefficient, k_{rc}, through:

$$\lambda_c = k\frac{k_{rc}}{\mu_n + \mu_w}. \tag{10}$$

The definition of the cross coefficient is somewhat arbitrary. As shown subsequently, the one proposed here is not only dimensionless, but also restricts the range of k_{rc} to $O(1)$ bounds with varying viscosity ratios. It also permits the definition of a symmetric relative permeability matrix.

Rose (1969, 1972) as well as subsequent authors (deGennes, 1983) who proposed such corrections presumed that all the permeability coefficients were functions only of saturation; no dependency on viscosities was discussed. Raats and Klute (1968) have also derived the relationships of Eqs. 7 and 8. They, however, do not presume symmetry and do not discuss how the coefficients would vary with either the saturation or viscosity ratio. In contrast, attempts to correct Darcy's two-phase equations for the presence of drag at fluid-fluid interfaces by including a viscosity ratio dependence on relative permeabilities have been proposed (Yuster, 1951). Indeed, nonwetting-phase permeabilities exceeding single-phase values have been measured (Odeh, 1959), indicating "lubrication" by a thin wetting-phase film surrounding the pore walls (Figure 1). A consistent

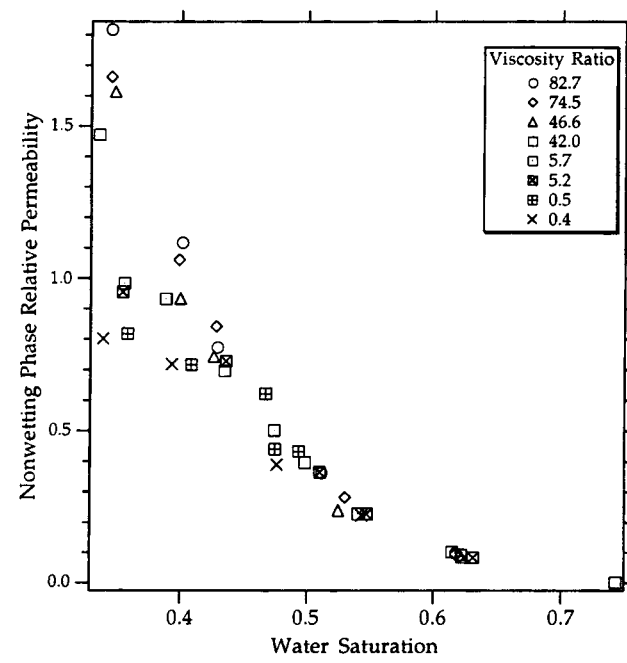

Figure 1. Experimental results showing dependence on nonwetting-phase relative permeability on viscosity ratio (after Odeh, 1959).

picture on the role and magnitude of the lubrication effect, however, has not emerged in the literature. Scott and Rose (1953), for example, showed that Yuster's (1951) model may overemphasize lubrication. They found that with modifications to the surface area parameters the lubrication effect is minor and that the relative permeability may never exceed one. In Yuster's (1951) model, apart from the difficulty of conceiving a stable distribution for the fluids, the nonwetting phase does not contact the solid. Hence, it could move with an infinite velocity as $\mu_w \to 0$, in contradiction with experimental data including those of Odeh (1959). Experimental data of Odeh (1959) have also been contested due to unknown clay effects (Downie and Crane, 1961). Danis and Jacquin (1983) and Danis and Quintard (1984) have reexamined lubrication. They used pore cross sections with corners and show that the stagnant zones of the wetting fluid can enhance permeability of the nonwetting fluid and that this effect depends on the details of the pore geometry.

Since the modeling of two-phase flow in porous media is of immense practical importance, several recent studies have reexamined the influence of shear induced momentum transport across interfaces. Bourbiaux and Kalaydjian (1988) calculated relative permeabilities from cocurrent and countercurrent flow experiments which differed substantially. They claimed that this is due to the presence of finite cross coefficient, unaccounted for in data interpretation. Therefore, through data fitting they could calculate cross coefficients as a function of saturation so that the diagonal relative permeability coefficients remained the same in the two experiments. Only saturation dependence of the three coefficients is discussed by them. On the theoretical side, Whitaker (1986) has applied volume-averaging methods to deduce governing equations for immiscible two-phase flow. The form he presents differs from the ones given here. Symmetry of the coefficients is not indicated, and his order of magnitude analysis suggests that the diagonal coefficients are independent of viscosity ratio although the off-diagonal terms may be present. Rothman (1990) used an immiscible lattice gas algorithm to calculate four permeability coefficients. No symmetry assumption was made to start with. By the nature of the algorithm, he was limited to studying flow through a channel with a rigid solid block in the center. His calculations show that the off-diagonal mobilities are *approximately* equal. No dependence of the permeability coefficients on viscosity was discussed by him.

The proposed modifications to the Darcy equations may thus be classified into two types: (i) the inclusion of a saturation-dependent cross term; (ii) a modification of the relative permeability coefficients to include viscosity ratio dependence. No definitive and well accepted form has emerged, and opinion is still divided about the importance of modifications to the extended Darcy equations.

In this article, we intend to address the above mentioned issues through extensive numerical modeling. We divide the effect of momentum transfer into lubrication and shear-induced flow which gives rise to off-diagonal coefficients. For our numerical model, we address the issue of symmetry of the permeability coefficient matrix and the dependence of permeability coefficients on viscosity ratio. Although the origin of the two effects is the same, it is important to distinguish the separate manifestations. For shear-induced flow, macroscopic transport of the second phase occurs across the medium, and so fluids' connectivity across the sample is important. For lubrication, it is only necessary that fluid interfaces occur parallel to the direction of flow. The interfaces may be present in isolation in each pore, for instance. It is, however, easy to see that if k_{rc} is nonzero, lubrication must occur.

The pore geometry in the numerical model is presented first. It has corners so that *steady* simultaneous two-phase flow within a pore is possible. Only stable fluid interface configurations with the contact angle $\theta = 0$ are considered in each pore. Using finite elements for each of these configurations we solve for pore flow conductances. We then construct a three-dimensional network of pores with the same cross-sectional geometry but differing sizes. A percolation algorithm for drainage, that is, invasion of nonwetting-phase into a wetting-phase filled medium, is then applied to the network. The phase saturations in each of the pores for the capillary pressure of interest are calculated. Thus, all the pore flow conductances are known. The problem is reduced to one of a resistor network except that two fluids may flow simultaneously. The resulting network is then solved to obtain both the relative permeabilities and the cross coefficients. The redundancy in the calculations is used to check for symmetry.

Single-Pore Model

We choose the four-cusp duct, shown in Figure 2, as the cross-section for the pores of the medium. Such a duct was thought to be representative of pore throats in a face-centered cubic packing of spheres. Moreover, at steady state, macroscopic amounts of wetting and nonwetting phases may also be simultaneously present in such pores. As the wetting-phase saturation decreases due to an increase in capillary pressure, the area of the fluid-fluid interface will decrease.

Single-pore capillary equilibrium

The invasion of nonwetting phase into a single pore is con-

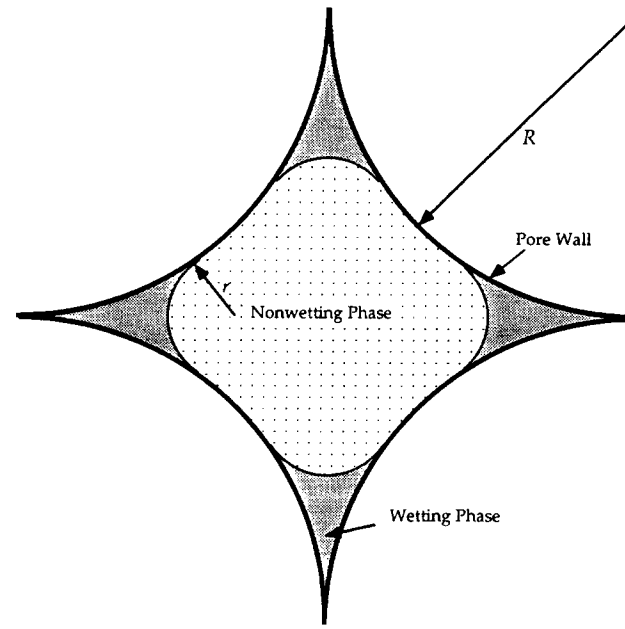

Figure 2. Cross section of a pore at entry capillary pressure.

trolled by the capillary pressure $p_n - p_w$ (Dullien, 1979). For a fluid-fluid interface in equilibrium, the capillary pressure is given by the Laplace equation (Defay and Prigogine, 1966);

$$p_c = 2\gamma\mathcal{H}, \tag{11}$$

where γ is the interfacial tension and $\mathcal{H}$ is the mean curvature of the interface. For the pore cross section of Figure 2 with contact angle equal to zero, the least interfacial curvature is obtained by a spherical cap whose radius is that of the inscribed circle of the pore. This may be thought to be the least capillary pressure needed for intrusion into the pore. Lenormand et al. (1983), however, showed that for a capillary with a rectangular cross section, the actual nonwetting-phase entry pressure was slightly lower than that predicted by allowing the largest possible radius of curvature. This has to do with the shape of the intruding interface. The ratio of the two pressures is nearly one and is about 0.943 for a pore of square cross section. We assume that this value is also valid for a four-cusp duct. To intrude into a duct of size R as shown in Figure 2, a capillary pressure

$$p_c = \frac{1.886\gamma}{(\sqrt{2}-1)R} \tag{12}$$

is therefore needed. Once this entry pressure criterion is met, nonwetting phase moves into the pore. After the nonwetting phase occupies the pore, the location of its meniscus r is determined from capillary equilibrium:

$$\frac{\gamma}{r} = p_c. \tag{13}$$

Note that in this equation account has been taken of the fact that one of the principal radii of curvature is infinite and the other has a radius r. The configuration of the meniscus after it has just been invaded is shown in Figure 2. The saturation S_w corresponding to this is approximately 0.2. With a subsequent increase in the capillary pressure, S_n will increase and the wetting fluid will recede further into the cusps. Thus, in any pore, nonwetting-phase saturation is either zero or some value greater than or equal to that corresponding to the entry capillary pressure.

Two-phase flow in a duct

The mean velocity, $\langle u \rangle$ of a Newtonian fluid through a four-cusp duct is:

$$\langle u \rangle = \frac{2d_h^2 \Delta p}{\mu\kappa l} \tag{14}$$

where l is the length of the duct, d_h is the effective hydraulic diameter given by:

$$d_h = \frac{2(4-\pi)R}{\pi}, \tag{15}$$

and κ is the friction coefficient. For laminar flow, it is 26.42 (Blevins, 1984).

For two-phase flow through the duct, we make some simplifications. First, we impose a capillary pressure with which we fix the configurations of the two fluids according to Eq. 11. The velocities are sufficiently small that any viscous flow pressure drop through the duct is negligible in relation to p_c, so that the interfacial configuration is unaltered through the length of the tube. Since p_c does not enter any of the mobility calculations, this also means that the interfacial configuration may be chosen directly by varying $\mathcal{H}$. Figure 3 represents one quarter of a four-cusp duct at an arbitrary capillary pressure. The curve joining point 3 with point 5 is the position of the interface. Lines 1-4 and 1-6 are the duct center lines. It should be noted from Figure 3 that there is symmetry about line 1-2. Hence, only one eighth of the duct need to be modeled. With point 1 as the origin, and lines 1-6 and 1-4 coinciding with the y and z axes, respectively, the following formulas give the coordinates (y,z) with the point number denoted by subscript:

$$(y,z)_1 = (0,0), \tag{16a}$$

$$(y,z)_2 = \left(\frac{2-\sqrt{2}}{2}R, \frac{2-\sqrt{2}}{2}R\right), \tag{16b}$$

$$(y,z)_3 = \left(\frac{Rr}{R+r}, \frac{R(a+r)}{R+r}\right), \tag{16c}$$

$$(y,z)_4 = (0,R), \tag{16d}$$

and

$$(y,z)_5 = (0,a+r), \tag{16e}$$

where

$$a = R - \sqrt{(R+r)^2 - R^2}.$$

We now make a further simplification in the single duct flow

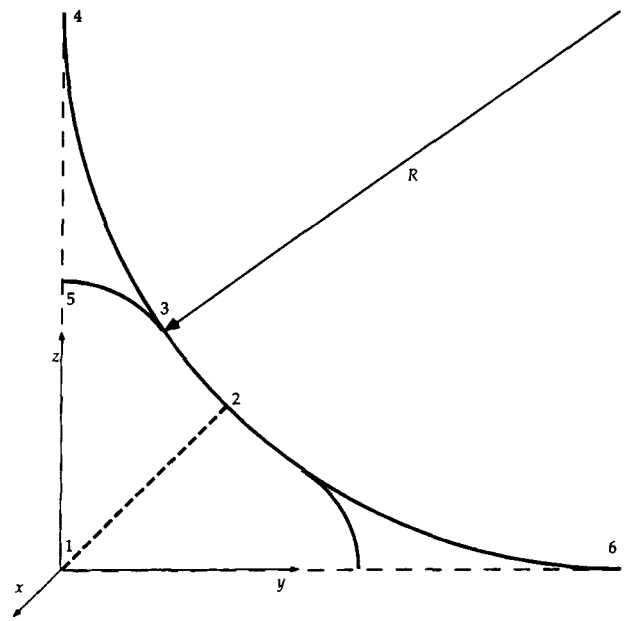

Figure 3. Quarter of the pore with boundary points.

model. Only unidirectional flow along the length of the pore is considered. Any circulation of fluid within a single pore is therefore ignored. As above, denoting the fluid velocities as u we have within each pore (Batchelor, 1967):

$$\frac{\partial p_w}{\partial x}+\mu_w\left[\frac{\partial^2 u_w}{\partial y^2}+\frac{\partial^2 u_w}{\partial z^2}\right]=0, \tag{17}$$

and

$$\frac{\partial p_n}{\partial x}+\mu_n\left[\frac{\partial^2 u_n}{\partial y^2}+\frac{\partial^2 u_n}{\partial z^2}\right]=0. \tag{18}$$

Obviously the x-axis is along the length of the pore. Since the flow is incompressible, due to continuity, the velocities u are independent of x. Since the pressures p_w and p_n are independent of y and z, both $(\partial p_w/\partial x)$ and $(\partial p_n/\partial x)$ are constants. The boundary conditions are that for each fluid, we satisfy no slip along the solid boundary curve 2-3-4. Along symmetry lines 1-4 and 1-2, the normal derivatives of velocities are zero. At the interface curve 3-5, velocities u_w and u_n are equal. The normal component of the force balance at the interface is irrelevant, because the interface is held stationary with the Laplace equation satisfied. The tangential component, however, is:

$$[\mu_n \nabla u_n-\mu_w \nabla u_w]\cdot n=0, \tag{19}$$

where n is the unit normal to the interface.

To solve Eqs. 17 and 18, we resort to a finite element method. The package MODULEF (1986) was used to solve for the velocity at each node. Figure 4 shows the constructed grids at the entry capillary pressure for which $S_w=0.2$. The wetting-phase saturation is determined by:

$$S_w=\frac{4}{(4-\pi)}\left[\sqrt{2\alpha+\alpha^2}-\beta-\alpha^2\left(\frac{\pi}{2}-\beta\right)\right], \tag{20}$$

where

$$\alpha=\frac{r}{R} \quad \text{and} \quad \beta=\sin^{-1}\frac{\sqrt{2\alpha+\alpha^2}}{1+\alpha}.$$

Analogous to the relative permeability and cross coefficients, wetting- and nonwetting-phase flow rates, q_w and q_n, through each pore may be represented in the form:

$$q_w=-\frac{g_{rw}}{\mu_w}g\Delta p_w-\frac{g_{rc}}{\mu_w+\mu_n}g\Delta p_n, \tag{21}$$

and

$$q_n=-\frac{g_{rc}}{\mu_w+\mu_n}g\Delta p_w-\frac{g_{rn}}{\mu_n}g\Delta p_n. \tag{22}$$

g/μ is the single-phase "conductance" of a given pore, which is known once the size R is fixed. The rest of the g coefficients are clearly functions of saturation within the pore but are independent of R. To determine g_{rw}, g_{rn}, and g_{rc} from the finite element calculations, we solve the model twice. We first hold $\Delta p_w=0$ and $\Delta p_n\neq 0$. The flow rates are obtained by integrating

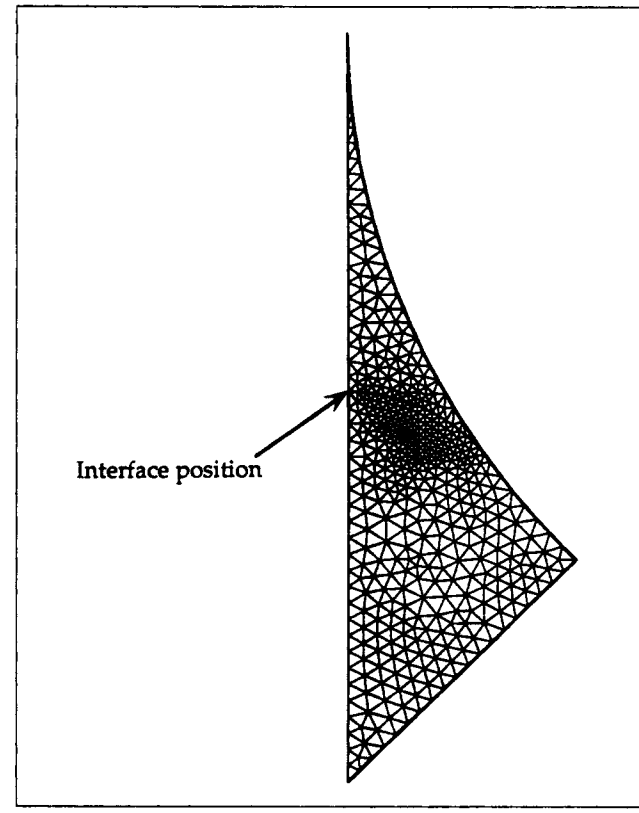

Figure 4. Finite element grids for $S_w=0.2$.

the fluid velocities over the area of the pore. From the calculated q_n and q_w, we obtain g_{rn} and g_{rc}, respectively. The calculation with $\Delta p_w\neq 0$ and $\Delta p_n=0$ similarly yields g_{rw} and g_{rc}. Reciprocity was thus used to verify the numerics. Within the computing precision it was found to be always satisfied. In addition, single-phase calculation was consistent with the friction coefficient of Eq. 14. Figure 5 shows the contours of u_n and u_w for a unit viscosity ratio.

For a fixed R, the calculations were performed for a number of different saturations and viscosity ratios. Saturations were changed by varying r. Numerical checks were made to ensure that g_{rn}, g_{rw}, and g_{rc} did not depend on viscosities themselves but only on the viscosity ratio $M=\mu_n/\mu_w$. The dependency of the relative and cross conductances on S_w and M is shown in Figures 6, 7 and 8.

For individual ducts, the range of saturations is limited by the value of the saturation at the entry capillary pressure. This is not a limitation to obtaining relative permeabilities and cross coefficients. Clearly, a model with a distribution of pore radii R will have to be considered. Apart from minor finite network-size effects, it should be possible to generate these curves spanning the full range of S_w. This model could take the form of a bundle of parallel tubes or a network of tubes on a lattice. The parallel model will not represent "tortuosity." The network would exhibit increasing tortuosity to a phase with decreasing saturation. This is more representative of a real porous medium.

Network Model

Network models that predict behavior in porous media were

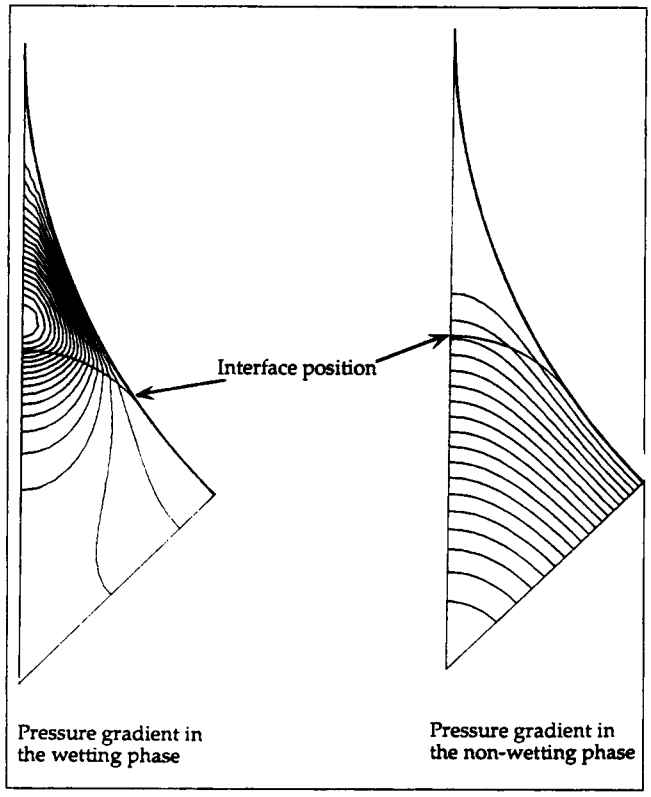

Figure 5. Velocity contours at $S_w = 0.2$.

used first by Fatt (1956) who used an equivalent resistor network to calculate properties like capillary pressure, relative permeabilities, and resistivity. Since then, numerous studies have been carried out with increasingly sophisticated rules to describe capillary equilibrium and simultaneous flow of fluids. There have also been analytical methods based on the percolation theory (Broadbent and Hammersley, 1957). To our knowledge, none of these studies has attempted to calculate cross coefficients for a network of pores.

In the present application, we construct an idealized porous medium using a network of *bonds*. The bonds coincide with

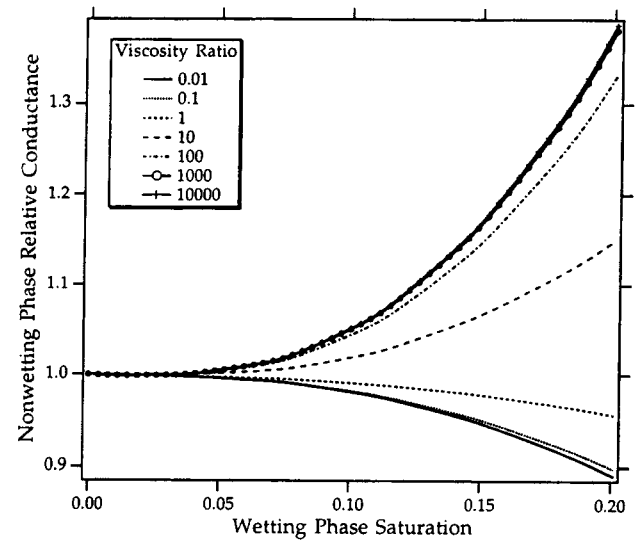

Figure 7. Nonwetting-phase pore relative conductance.

the *edges* on a graph obtained from a simple cubic lattice, the vertices of the graph being the nodes of the bonds. Physically, the bonds represent the pores, each having the cross section of the four cusp duct considered in the previous section. Its size R is selected at random from a log-normal distribution. In a numerical model, it is possible to contrive varied pore lengths l in a regular lattice as was done by Fatt (1956). We, however, used the same l for all pores.

Since the four cups pores permit the presence of two phases simultaneously, some rules need to be implemented regarding phase connectivity at the nodes. We ignore the physical details of connections at the nodes and simply assume that both phases may be connected across a node simultaneously. *Thus, the wetting phase remains connected throughout the medium at all saturations*. Such a construction is topologically equivalent to the *bond percolation* problem (see, for example, the review of Shante and Kirkpatrick, 1971). Because of biphasic continuity across the nodes, the effect of momentum transfer through the interface may be overestimated.

As in the single-pore flow calculation, we first establish

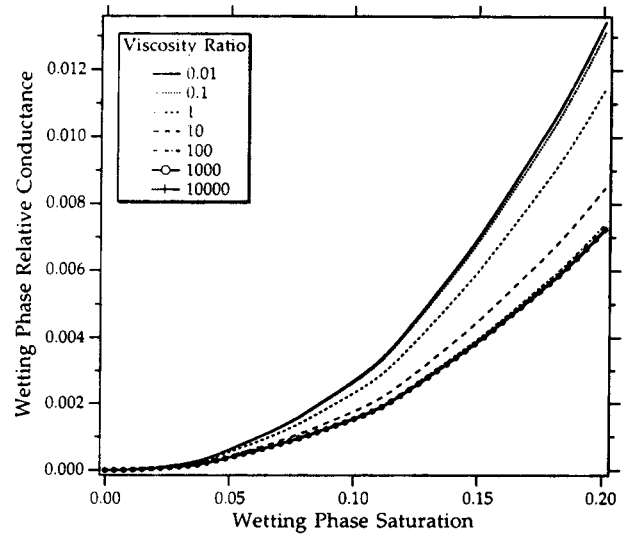

Figure 6. Wetting-phase pore relative conductance.

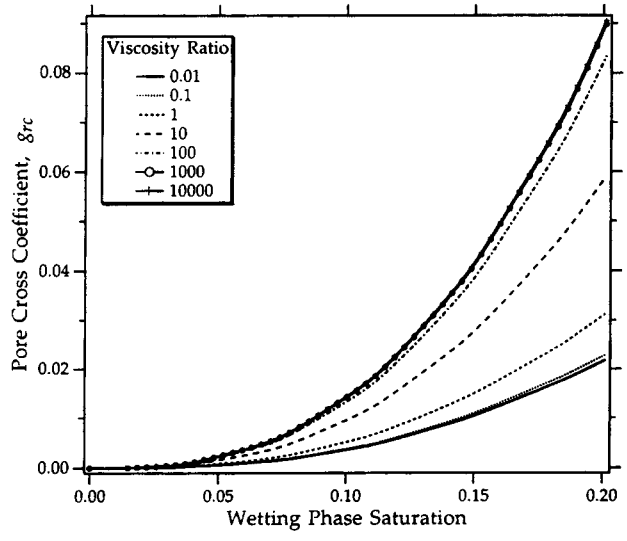

Figure 8. Pore cross coefficient.

capillary equilibrium across the network. The invading fluid enters through one of the faces and is allowed to exit through the opposite face. Periodic boundary conditions are applied to the other four faces of the network. This is done by connecting the two rows of bonds on the opposite faces with an additional layer of bonds, perpendicular to the faces. Thus, orthogonal to the inlet and exit faces, the lattice is pseudo-infinite.

The algorithm used to determine equilibrium fluid distribution as a function of capillary pressure, or r is a variation of the ordinary percolation algorithm. In the context of multiphase distribution, a similar algorithm was used first by Chatzis and Dullien (1977). A flowchart of the algorithm implemented here is given by Figure 9. Only initial drainage is considered in all of the numerical experiments. Since snap-off mechanism as considered by Mohanty and Salter (1982) is not accounted for, provision to account for the trapping of the nonwetting phase is unnecessary. Clearly, wetting phase remains connected at all capillary pressures because of its presence in all the pores.

The algorithm begins with the network initially saturated by the wetting phase. Nonwetting phase is invaded into the network by increasing the capillary pressure, p_c to the entry pressure of the largest, unaccessed bond on the interface. All bonds which subsequently come onto the interface and can be entered at that value of the capillary pressure are entered according to the steps in Figure 9. These are irreversible Haines' (1930) jumps. The algorithmic step for the occupation of these pores corresponds exactly to the analytic method of Ramakrishnan and Wasan (1986) for initial drainage. In both methods, irreversible jumps occur essentially in one step. Due to the wetting phase being continuous, the equilibrium configuration will correspond exactly to that obtained by the invasion percolation of Wilkinson and Willemsen (1983), where invasion proceeds in an ordered sequence. The process is continued with increasing p_c until the nonwetting phase reaches the outlet face, at which point macroscopic transport of both fluids across the network is possible. This is when a fraction of pores equal to the critical percolation probability is allowed to be occupied by the criterion of capillary pressure alone without any regard to whether these pores are accessible from the boundary of the inlet face (Wilkinson and Willemsen, 1983; Ramakrishnan and Wasan, 1986; Heiba et al., 1992). For an infinite network of pores at breakthrough, $S_n = 0$. For a finite system, S_n scales as some inverse power of N, where N is the number of bonds in the lattice from inlet to outlet. From recent estimates (Clerc et al., 1990) of fractal dimension of a percolating fluid at breakthrough, we know that in 3-D,

$$\phi_n \sim \beta N^{-0.477}, \tag{23}$$

where β depends on the details of the network such as the pore size distribution and the type of lattice. As a check, we varied our network size from $5\times5\times5$ to $30\times30\times30$ in steps of five and obtained the best least-square fit of the exponent to be 0.45, in reasonable agreement with the Clerc et al. (1990) result. Our value was obtained by averaging 50 realizations for each size.

For all capillary pressures above percolation threshold, the velocities v_n and v_w due to an applied pressure gradient can be determined for each phase. By comparing these results to the

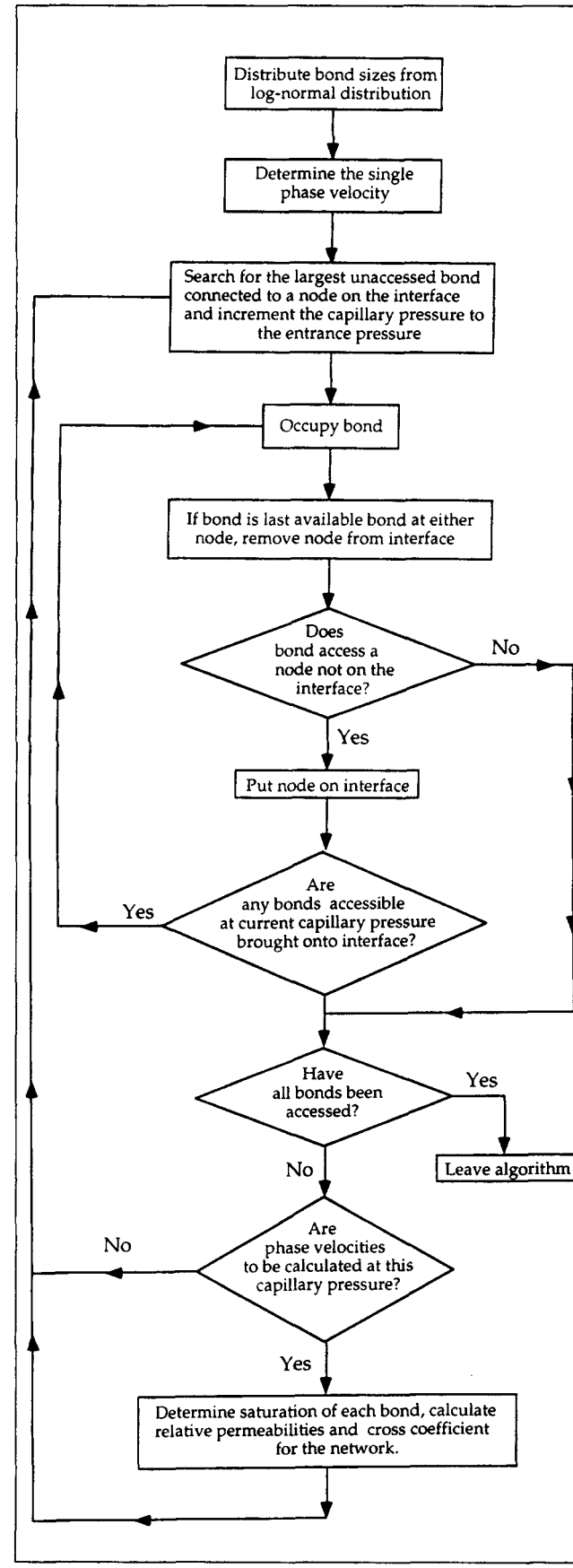

Figure 9. Percolation algorithm.

single-phase velocity calculations, relative permeabilities and cross coefficients are obtained. We do this by first setting $\Delta p_w \neq 0$ and $\Delta p_n = 0$. The pressure drop is meant to be small enough that capillary equilibrium is left unaffected in every pore. Although such an experiment is difficult to achieve in practice with liquid flow in a multitude of pores, a numerical experiment is carried out without any difficulty. Physically, it will correspond to reaching capillary pressure equilibrium through the rock and subsequently imposing an infinitesimal pressure drop in one of the fluids. The resulting velocities then give the direct and the cross-mobility coefficients at the saturation corresponding to the capillary pressure. Numerically, the wetting and nonwetting fluxes are determined through a system of equations:

$$q_w^{ij} = -\frac{g_{rw}(S_w^{ij}; M)}{\mu_w} g^{ij} \Delta p_w^{ij} - \frac{g_{rc}(S_w^{ij}; M)}{\mu_w + \mu_n} g^{ij} \Delta p_n^{ij}, \quad (24)$$

and

$$q_n^{ij} = -\frac{g_{rc}(S_w^{ij}; M)}{\mu_w + \mu_n} g^{ij} \Delta p_w^{ij} - \frac{g_{rn}(S_w^{ij}; M)}{\mu_n} g^{ij} \Delta p_n^{ij}, \quad (25)$$

where the superscript ij refers to a bond connecting adjacent nodes i and j. Knowing S_w^{ij}, the values of g_{rw}, g_{rn}, and g_{rc} are obtained from the interpolation of the lookup table constructed from the single-duct finite element calculation. g^{ij} depends on R, and from Eq. 14 it is:

$$g^{ij} = \frac{8(4-\pi)^3 (R^{ij})^4}{\kappa l \pi^2}. \quad (26)$$

Using Eqs. 24 and 25 and flux conservation at each node i:

$$\sum_j q_w^{ij} = 0 \quad \text{and} \quad \sum_j q_n^{ij} = 0, \quad (27)$$

we form a system of equations for unknowns p_w and p_n at each node. The resulting system of linear equations forms a sparse, nonsymmetric coefficient matrix. The most efficient algorithm to solve the system was an LU preconditioned Orthomin method (Vinsome, 1976), as implemented in SLAP (Seager and Greenbaum, 1988). Knowing the pressures, Eqs. 24 and 25 give the fluxes. Thus, the total wetting- and nonwetting-phase fluxes Q_w^w and Q_n^w through the inlet and exit faces may be determined. The same calculation is then repeated with $\Delta p_n = 1$ and $\Delta p_w = 0$ to get Q_n^n and Q_w^n. Repeating the calculation with just a single phase of viscosity μ for a $\Delta p = 1$, we also calculate the single phase flow rate Q. Then,

$$k_{rw} = \frac{Q_w^w}{Q} \frac{\mu_w}{\mu}$$

$$k_{rc} = \frac{Q_n^w}{Q} \frac{\mu_w + \mu_n}{\mu} = \frac{Q_w^n}{Q} \frac{\mu_w + \mu_n}{\mu}. \quad (28)$$

$$k_{rn} = \frac{Q_n^n}{Q} \frac{\mu_n}{\mu}$$

Again redundancy in the calculation of k_{rc} is used to verify some of the numerics. As expected, symmetry was always satisfied.

For each successively smaller r, the computations are repeated. They are also performed for a number of viscosity ratios M. To examine the artifacts of using a finite-sized network, the lattice size was fixed at $N \times N \times N$, and 500 realizations were carried out and the results averaged. Little lattice-size effects were apparent for k_{rw}, k_{rn}, and k_{rc}. For all the results presented below, we used an average of ten realizations on a $30 \times 30 \times 30$ lattice.

Results and Discussion

Relative permeability and cross-coefficient curves were generated using the network model at a number of viscosity ratios. The same ten realizations were used for all of the viscosity ratios. Although k_{rw}, k_{rn}, and k_{rc} do not show finite-size effects at most of the saturations, the nonwetting phase does not traverse the network, until it reaches a finite saturation. Thus, k_{rn} and k_{rc} are zero until this saturation is reached. To overcome this problem, k_{rn} and k_{rc} were calculated only for $S_w \leq 0.9$, where finite-size effects were absent and then extrapolated up to $S_w = 1.0$ using a tension spline (Cline, 1974).

Lubrication

We shall reserve the term "lubrication" to denote the alteration of the diagonal relative permeability coefficients with viscosity ratio. The numerical curves for k_{rw} and k_{rn} are shown in Figures 10 and 11. It is evident that the lubrication effect is stronger on k_{rn} than on k_{rw}. The main reason for this is that a bulk of the wetting-phase transport occurs through pores completely occupied by it where there are no fluid-fluid interfaces to manifest lubrication. But, all pores with the nonwetting phase contain the wetting phase. Here, the interfaces do play a role in determining nonwetting-phase velocity.

The numerical computations are in qualitative agreement with the experimental results of Odeh (1959) referred to earlier. Despite the nature of the calculations performed in this article which may tend to overestimate lubrication, quantitatively we find the effect to be smaller than what was measured by Odeh (1959). Also, Odeh's k_{rn} curves do not show a maximum. This

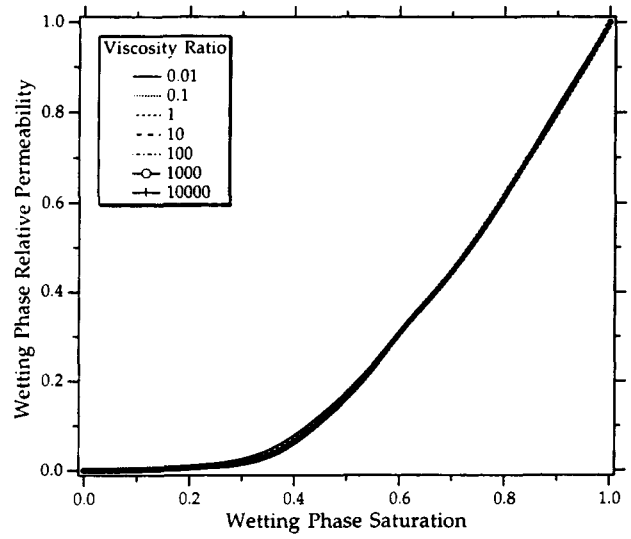

Figure 10. Wetting-phase relative permeability for different viscosity ratios.

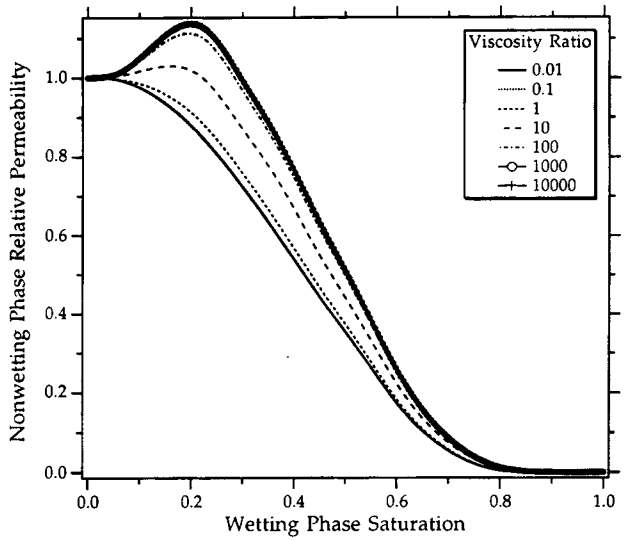

Figure 11. Nonwetting-phase relative permeability for different viscosity ratios.

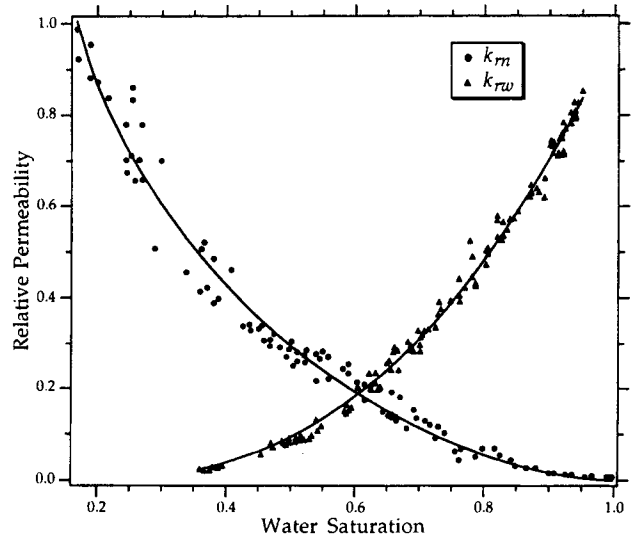

Figure 12. Water and gas relative permeability for an unconsolidated sand (after Wyckoff and Botset, 1936).

might have to do with the fact that his experimental data do not go down to sufficiently low water saturation. Unlike the network model, in real systems it is possible for the wetting phase on the pore surface to lose macroscopic continuity across the network, which leads the wetting phase to become effectively trapped. The curves of Figure 10 should be limited to some trapped-water saturation as the lower limit.

The lubrication effect reaches a limit for both small and large viscosity ratio. The limit is lower than that observed in the single-duct modeling. Obviously, the random nature of the bond radii in the network implies that a portion of the nonwetting-phase transport occurs through pores where it comes in contact with a significant amount of solid surface. Even at the limit of infinite M, the velocity of the nonwetting fluid is limited by the presence of the solid/nonwetting fluid interfaces. Conversely, for $M=0$, k_{rn} approaches the limit where lubrication is absent.

At this point, it is useful to mention some of the other experimental data available in the literature. Wyckoff and Botset (1936) performed experiments on unconsolidated sand packs with water and gas simultaneously flowing through the pack. The value of M was approximately 0.015. One of their data-set is reproduced in Figure 12. In this set, the lowest water saturation reached was 0.2, at which point oil relative permeability close to one was obtained. It is obvious that the numerical calculations of ours is in qualitative agreement with their data. Wyckoff and Botset (1936) also performed experiments in which they varied liquid viscosity and found no appreciable difference in the results, especially for the wetting-phase (liquid) relative permeability. Similar findings have been reported by Krutter (1941), who used oil as a wetting phase and varied its viscosity from 0.002–0.1 Pa·s. Osoba et al. (1951) also discuss similar data. Clearly, this is to be expected from our calculations. At low M sensitivity to the viscosity ratio is diminished, and k_{rw} has little dependency at all on M.

Cross coefficient

The cross coefficient as a function of viscosity ratio and saturation is shown in Figure 13. The obvious conclusion is that k_{rc} is not small for all saturations in comparison with the relative permeabilities and cannot be neglected arbitrarily as is done in practice today. As with k_{rn}, there is a strong viscosity ratio dependence. The definition of k_{rc} as given by Eq. 10 is appropriate. It leads to reasonable upper and lower limiting curves as the viscosity ratio is varied.

Kalaydjian et al. (1989) measured relative permeabilities and cross coefficients by conducting a sequence of experiments. The viscosity ratio was about 11.5. γ-ray adsorption was used to measure saturation profiles within the sample, and capillary pressure along the rock sample was also measured. By carrying out numerical simulations with a matrix of permeabilities, they back calculated the coefficients. Since their results are all specific to the sandstone they chose and were obtained for imbibition, only qualitative comparison with our numerical computations is possible. Accordingly, we note from their Figure 10 that the cross coefficient goes through a maximum

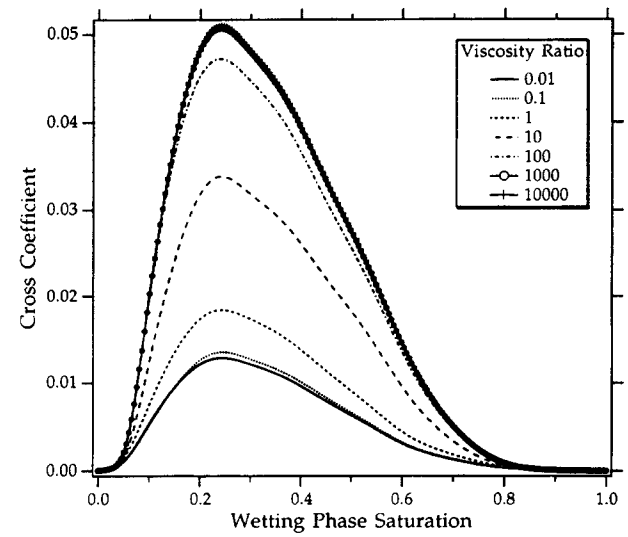

Figure 13. Cross coefficients for different viscosity ratios.

at some intermediate saturation as our computations suggest. It is zero at either end of the saturation range. Furthermore, when their coefficients are reinterpreted in terms of k_{rc}, the maximum is close to 0.04, in excellent agreement with the value indicated in Figure 13.

The functional dependence of the lubrication effect of k_{rn} $[k_{rn}(S_w; M) - k_{rn}(S_w; M=0)]$ on viscosity ratio and saturation is very similar to that of k_{rc}. The reason for this is that both of these have the same origins. All the fluid-fluid interfaces contribute to lubrication and off-diagonal terms. It is, however, possible that in real media, once the wetting phase begins to get macroscopically disconnected, the off-diagonal terms may diminish. Lubrication, however, will not diminish.

Based on the results of this article it is natural to suggest the following governing equations for the two-phase creeping flow in porous media:

$$v_w = -\frac{kk_{rw}(S_w; M)}{\mu_w} \nabla p_w - \frac{kk_{rc}(S_w; M)}{\mu_w + \mu_n} \nabla p_n \qquad (29)$$

and

$$v_n = -\frac{kk_{rc}(S_w; M)}{\mu_w + \mu_n} \nabla p_w - \frac{kk_{rn}(S_w; M)}{\mu_n} \nabla p_n \qquad (30)$$

Summary and Conclusions

- A network model based on a four-cusp pore has been used to generate two-phase fluid transport coefficients. Within each pore, a finite element calculation was used to generate conductances which were then used in the context of the network calculation.
- A network model was used to simulate invasion of nonwetting phase using a percolation-like algorithm. The model assumes a network of bonds with biphasic continuity at the nodes. Assuming capillary equilibrium, both relative permeabilities and cross coefficient were calculated for varying saturations at different viscosity ratios.
- As expected, the transport coefficients are strong functions of saturation. But they also show $O(1)$ variation with respect to viscosity ratio. k_{rw}, however, shows only a weak dependence on the viscosity ratio.
- In general, the presence of the cross coefficient implies a viscosity ratio dependence for all the transport coefficients. The converse is not necessarily true when wetting phase gets disconnected. k_{rn} may show dependence on M, but k_{rc} may be negligible.
- The definition of k_{rc} as given leads to $O(1)$ variation, as M goes from zero to infinity.

Acknowledgment

The authors thank Schlumberger for permission to publish this article.

Literature Cited

Barenblatt, G. I., V. M. Entov, and V. M. Ryzhik, *Theory of Fluid Flows through Natural Rocks*, Kluwer Academic Publishers, Boston (1990).

Batchelor, G. K., *An Introduction to Fluid Dynamics*, Cambridge Univ. Press, Cambridge (1967).

Bear, J., *Dynamics of Fluids in Porous Media*, Elsevier, New York (1972).

Blevins, R. D., *Applied Fluid Dynamics Handbook*, Van Nostrand Reinhold, New York (1984).

Bourbiaux, B. J., and F. J. Kalaydjian, "Experimental Study of Cocurrent and Countercurrent Flows in Natural Porous Media," Technical Conf. and Exhibition of SPE, Houston (1988).

Broadbent, S. R., and J. M. Hammersley, "Percolation Processes: 1. Crystals and Mazes," *Proc. Cambridge Phil. Soc.*, **53**, 629 (1957).

Buckingham, E., "Studies on the Movement of Soil Moisture," *U.S. Dept. of Agriculture, Bureau of Soils-Bull.*, **38**, 1 (1907).

Callen, H. B., *Thermodynamics*, Wiley, New York (1960).

Chatzis, I., and F. A. L. Dullien, "Modelling Pore Structure by 2-D and 3-D Networks with Application to Sandstones," *J. Can. Pet. Technol.*, **16**, 97 (1977).

Clerc, J. P., G. Giraud, J. M. Laugier, and J. M. Luck, "The AC Conductivity of Binary Disordered Systems, Percolation Clusters, Fractals, and Related Models," *Adv. Phys.*, **39**, 191 (1990).

Cline, A. K., "Scalar- and Planar-valued Curve Fitting Using Splines Under Tension," *Comm. ACM*, **17**, 218 (1974).

Danis, M., and Ch. Jacquin, "Influence du Contraste de Viscosités sur les Perméabilitiés Relatives lors du Drainage Expérimentation et Modélisation," *Rev. Inst. Français Pétrole*, **38**, 723 (1983).

Danis, M., and M. Quintard, "Modélisation D'un Écoulement DiPhasique Dans Une Succession de Pores," *Rev. Inst. Français Pétrole*, **39**, 37 (1984).

Darcy, H., *Les Fontaines Publiques de la Ville de Dijon*, Victor Malmont, Paris (1856).

Defay, R., and I. Prigogine, *Surface Tension and Adsorption*, Wiley, New York (1966).

deGennes, P. G., "Theory of Slow Biphasic Flows in Porous Media," *Phys. Chem. Hydrody.*, **4**, 175 (1983).

Downie, J., and F. E. Crane, "Effect of Viscosity on Relative Permeability," *Soc. Pet. Eng. J.*, **1**, 59 (1961).

Dullien, F. A. L., *Porous Media, Fluid Transport and Pore Structure*, Academic Press, New York (1979).

Fatt, I., "The Network Model of Porous Media III Dynamic Properties of Networks with Tube Radius Distribution," *Pet. Trans. AIME*, **207**, 164 (1956).

Haines, W. B., "Studies in the Physical Properties of Soil V. Hysteresis Effect in Capillary Properties, and the Models of Moisture Distribution Associated Therewith," *J. Agri. Sci.*, **20**, 97 (1930).

Hassler, G. L., R. Rice, and E. H. Leeman, "Investigations on the Recovery of Oil from Sandstones by Gas Drive," *Trans. AIME*, **118**, 116 (1936).

Heiba, A. A., M. Sahimi, L. E. Scriven, and H. T. Davis, "Percolation Theory of Two Phase Relative Permeability," *SPE Res. Eng.*, **7**, 123 (1992).

Kalaydjian, F., B. Bourbiaux, and D. Guerillot, "Viscous Coupling between Fluid Phases for Two-Phase Flow in Porous Media: Theory Versus Experiment," *Europ. Symp. on Improved Oil Recovery*, Budapest, Hundary (1989).

Krutter, H., "Air Drive Experiments," *Prod. Monthly*, **6**, 25 (1941).

Lenormand, R., C. Zarcone, and A. Sarr, "Mechanisms of the Displacement of One Fluid by Another in a Network of Capillary Ducts," *J. Fluid Mech.*, **135**, 337 (1983).

Leverett, M. C., "Flow of Oil-Water Mixtures through Unconsolidated Sands," *Trans. AIME*, **132**, 149 (1939).

Leverett, M. C., "Capillary Behavior in Porous Solids," *Pet. Technol.*, **3**, 1 (1940).

Leverett, M. C., and W. B. Lewis, "Steady Flow of Gas-Oil-Water Mixtures through Unconsolidated Sands," *Trans. AIME*, **142**, 107 (1941).

Marle, C. M., *Multiphase Flow in Porous Media*, Gulf Publishing, Houston (1981).

MODULEF, A Library of Finite Elements, INRIA, France (1986).

Mohanty, K. K., and S. Salter, "Multiphase Flow in Porous Media: II. Pore-Level Modeling," *Technical Conf. and Exhibition of SPE and AIME*, New Orleans (1982).

Muskat, M., and M. W. Meres, "The Flow of Heterogeneous Fluids through Porous Media," *Physics*, **7**, 346 (1936).

Muskat, M., R. D. Wyckoff, H. G. Botset, and M. W. Meres, "Flow of Gas-Liquid Mixtures through Sands," *Trans. AIME*, **123**, 69 (1937).

Nutting, P. G., "Physical Analysis of Oil Sands," *Bull. Amer. Assoc. Petrol. Geol.*, **14**, 1337 (1930).
Odeh, A. S., "Effect of Viscosity Ratio on Relative Permeability," *J. Pet. Technol.*, **11**, 346 (1959).
Osoba, J. S., J. G. Richardson, J. K. Kerver, J. A. Hafford, and R. M. Blair, "Laboratory Measurements of Relative Permeability," *Trans. AIME*, **192**, 47 (1951).
Raats, P. A. C., and A. Klute, "Transport in Soils: The Balance of Momentum," *Soil Sci. Soc. Amer.*, **32**, 452 (1968).
Ramakrishnan, T. S., and D. T. Wasan, "Two-Phase Distribution in Porous Media: An Application of Percolation Theory," *Int. J. Multiphase Flow*, **12**, 357 (1986).
Richards, L. A., "Capillary Conduction of Liquids through Porous Mediums," *Physics*, **1**, 318 (1931).
Rose, W., "Transport through Interstitial Paths of Porous Solids," *METU J. Pure and Appl. Sci.*, **2**, 117 (1969).
Rose, W. D., *Fundamentals of Transport Phenomena in Porous Media*, IAHR, ed., p. 229, Elsevier Publishing, New York (1972).
Rothman, D. H., "Macroscopic Laws of Immiscible Two-Phase Flow in Porous Media: Results from Numerical Experiments," *J. Geophysical Res.*, **95**, 8663 (1990).
Scheidegger, A. E., *The Physics of Flow through Porous Media*, Univ. of Toronto Press, Toronto (1974).
Scott, P. H., and W. Rose, "An Explanation of the Yuster Effect," *J. Petrol. Tech.*, **5**, 19 (1953).
Seager, M. K., and A. Greenbaum, "SLAP: Sparse Linear Algebra Package," *Computer Software for the Solution of Large Linear Systems*, Lawrence Livermore National Laboratory (1988).
Shante, V. K. S., and S. Kirkpatrick, "An Introduction to Percolation Theory," *Adv. Phys.*, **20**, 325 (1971).
Vinsome, P. K. W., "Orthomin, an Iterative Method for Solving Sparse Banded Sets of Simultaneous Linear Equations," *Symp. on Numerical Simulation of Reservoir Performance*, preprint SPE 5279, Los Angeles (1976).
Whitaker, S., "Flow in Porous Media: II. the Governing Equations for Immiscible, Two-Phase Flow," *Trans. in Porous Media*, **1**, 105 (1986).
Wilkinson, D., and J. F. Willemsen, "Invasion Percolation: a New Form of Percolation Theory," *J. Phys. A: Math. Gen.*, **16**, 3365 (1983).
Wyckoff, R. D., and H. G. Botset, "The Flow of Gas-Liquid Mixtures through Unconsolidated Sands," *Physics*, **7**, 325 (1936).
Yuster, S. T., "Theoretical Considerations of Multiphase Flow in Idealized Capillary Systems," *World Petroleum Cong. Proc., Section II. Drilling and Production*, The Hague (1951).

Manuscript received Oct. 14, 1992, and revision received Dec. 28, 1992.